

Physicochemical Profiling of Sartans: A Detailed Study of Ionization Constants and Distribution Coefficients

by Paolo Tosco^{a)}, Barbara Rolando^{a)}, Roberta Fruttero^{*a)}, Yveline Henchoz^{b)}, Sophie Martel^{b)}, Pierre-Alain Carrupt^{b)}, and Alberto Gasco^{a)}

^{a)} Dipartimento di Scienza e Tecnologia del Farmaco, Università degli Studi di Torino, Via Pietro Giuria 9, I-10125 Torino (phone: +39011 6707850; fax: +39011 6707286; e-mail: roberta.fruttero@unito.it)

^{b)} Unité de Pharmacochimie, Section des sciences pharmaceutiques, Université de Genève, Université de Lausanne, 30 Quai Ernest Ansermet, CH-1211 Genève 4

A detailed investigation of the ionization and lipophilicity profiles of selected sartans (valsartan, losartan, irbesartan, candesartan, candesartan cilexetil), a class of antihypertensives commonly used in therapy, is presented. The pK_a macroconstants were determined by integrated potentiometry, capillary electrophoresis, and UV spectrophotometry. The measured pK_a macroconstants were connected with the ionizable centers present in each molecule with the aid of model compounds. Potentiometric titrations with the GLpKa apparatus were performed to determine the distribution profile ($\log D$ vs. pH) of valsartan, while the shake-flask procedure was used to characterize the distribution profile of the other compounds. Valsartan showed a lipophilicity profile consistent with the presence of two acidic centers. Losartan and irbesartan, which contain one acidic and one basic center, displayed the classical bell-shaped profile of ordinary ampholytes. By contrast, a more complex situation emerged in the case of candesartan, due to the large number of ionization equilibria involved. The low solubility of candesartan cilexetil, together with the ease of hydrolysis of the ester moiety, prevented a successful investigation of its ionization and lipophilicity profiles.

Introduction. – The lipophilicity of an ionizable compound can be measured as the partition coefficient P ($\log P$) between two essentially immiscible solvents related, by definition, to a well-defined electrical state. If the compound can exist in different electrical states, its lipophilicity is expressed by the distribution coefficient D ($\log D$). This latter molecular descriptor is the weighted mean of the lipophilicity of each electrical species under which the compound can exist in a pH-dependent proportion [1]. Since a drug has to cross several biomembranes during its random walk to the target, the bioavailability of an ionizable drug will depend on the pH of the environment in which biomembranes are located and on the pK_a value(s) of the drug. Therefore, it is important to know the lipophilicity profile of a drug, namely $\log D$ vs. pH, a key factor for the control of the pharmacokinetic and the pharmacodynamic phases of drug action [2][3]. These profiles have been studied for many drugs using, traditionally, the octanol/H₂O partition coefficients to model the partitioning in biomembranes.

Sartans are an important class of drugs acting as selective antagonists of angiotensin II (Ang II) at the AT₁ receptors. This antagonism is commonly used to treat hypertension, but additional therapeutic indications are emerging for these drugs such as the management of congestive heart failure, myocardial infarction, and diabetic

nephropathy [4]. Sartans commonly used in therapy are valsartan (**1**), losartan (**2**), irbesartan (**3**), candesartan (**4**), and candesartan cilexetil (**5**) (Fig. 1). The pK_a constants and the lipophilicity profiles of sartans have been studied only in a scattered and incomplete manner, and frequently with confusing and conflicting results [5]. This work is dedicated to a close investigation of the ionization constants and lipophilicity profiles of these drugs by the combined use of potentiometry, capillary electrophoresis (CE), and UV spectrophotometry. In addition to the sartan derivatives, selected tetrazoles and benzimidazoles were included in the study as model compounds (Fig. 2).

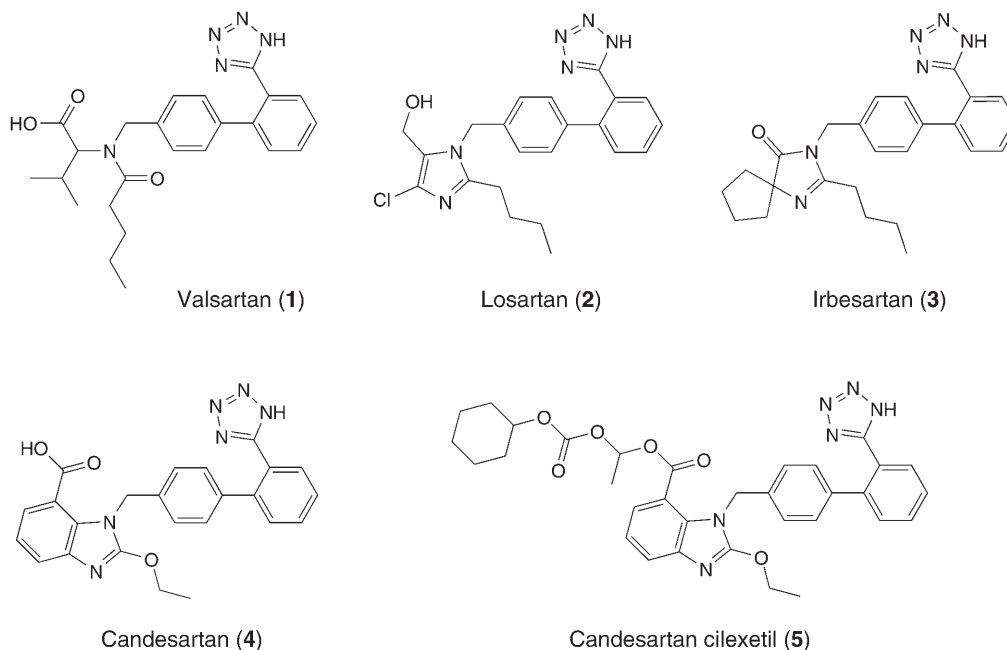


Fig. 1. Structures of compounds investigated

Results and Discussion. – The sartan drugs studied here, namely valsartan, losartan, irbesartan, candesaratan, and candesaratan cilexetil (**1–5**, resp.; Fig. 1), contain different ionizable fragments such as acidic functions (carboxy and tetrazole groups) or basic heterocyclic moieties (1*H*-imidazole, 4,5-dihydro-5-oxo-1*H*-imidazole, and 1*H*-benzimidazole rings). As a consequence, their complex ionization schemes lead to intricate lipophilicity profiles. Since sartans contain ionizable groups characterized by a small difference between equilibrium constants (low ΔpK_a values), they exist in several different electrical states depending on pH (as exemplified with the ionization equilibria of candesaratan (**4**) in Scheme 1). To know the exact equilibrium concentration of each electrical species at a fixed pH, it would be necessary to know all the microconstants k related to the equilibria between the individual forms. However, it is not possible to determine all the microscopic ionization constants due to their proximity. Therefore, all measured pK_a values in the stepwise approach used here

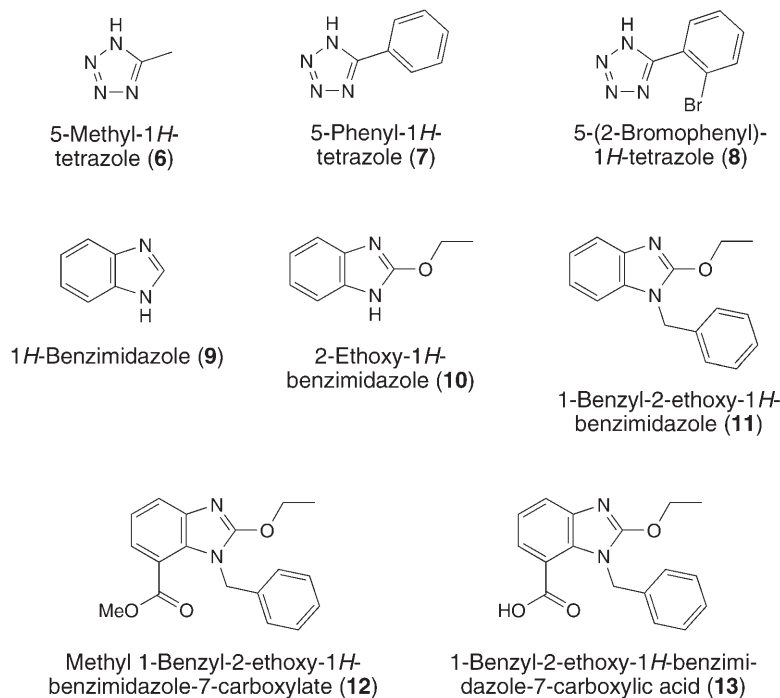
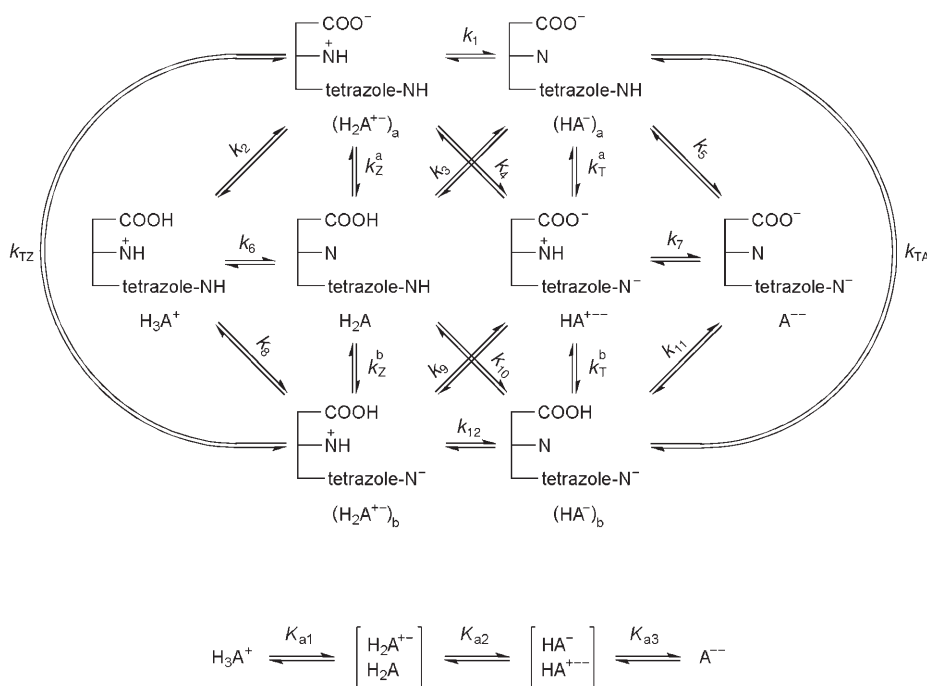


Fig. 2. Structures of some tetrazoles and benzimidazoles used as model compounds

to clarify the physicochemical profiles of sartans are macroconstants K , since they refer to their stoichiometric ionization. Experimental determinations were accomplished with potentiometric techniques; when the pK_a value to be assessed lied outside the range which can be determined potentiometrically, electrophoretic and spectrophotometric techniques were used, as mentioned below. The constants thus obtained were also used for the study of lipophilicity profiles. Only a few values for the ionization constants of the simple tetrazole models **6–8** are reported in literature ($pK_a(\text{tetrazole}) = 4.89$ [6], $pK_a(5\text{-methyltetrazole } \mathbf{6}) = 5.50$ [7], $pK_a(5\text{-phenyl-1}H\text{-tetrazole } \mathbf{7}) = 4.38$ [8]). Similarly, only two pK_a values of the 1*H*-benzimidazole models **9–13** studied herein are known ($pK_a(1H\text{-benzimidazole } \mathbf{9}) = 5.58$; $pK_a(2\text{-ethoxy-1}H\text{-benzimidazole } \mathbf{10}) = 4.39$ [9]). Since the methods used for these studies are not always comparable, we decided to measure the pK_a values of the reference compounds again under the same experimental conditions used for sartans (*Table 1*). The results obtained clearly demonstrate that the acidity of the tetrazole moiety increases with an aromatic 5-substitution, reflecting a larger delocalization of the negative charge over the aromatic cycle, together with the influence of the electron-withdrawing substituent in the case of **8**. The lipophilicity profiles of the two aromatic tetrazoles **7** and **8** confirm the charge delocalization with a low difference between the partition coefficients of neutral and ionized forms (see *Table 1*) [10][11]. The ionization constants for drugs **1–5** are collected in *Table 2*; the plots of weight-% of MeOH vs.

Scheme 1. Micro- and Macro-equilibria of Candestartan (4) Ionization


 Table 1. Ionization Constants and Lipophilicity Parameters of Model Compounds 6–13^{a)}

Compound	$pK_a^b)$	CLOGP ^{c)}	$\log P^{N^d)}$	$\log P^{I^e)}$	$diff(\log P^{N-I})$
6	5.44 ^{f)}	-0.83	-0.49	-	-
7	4.32 ^{f)g)}	0.99	1.50 ^{h)}	-0.94	2.44
8	3.87 ^{f)g)}	1.56	1.81 ^{h)}	-0.86	2.67
9	5.48 ^{f)}	1.57	-	-	-
10	4.30 ^{f)}	2.93	-	-	-
11	3.68 ^{f)g)}	4.41	-	-	-
12	2.38 ⁱ⁾	4.42	-	-	-
	ND ^{f)g)}				
	2.45 ⁱ⁾				
13	2.12 and 3.67 ⁱ⁾	4.40	-	-	-
	ND and 3.87 ^{f)g)}				

^{a)} ND: not determinable (see text for more details). ^{b)} Potentiometric method, standard deviation (SD) < 0.02; CE, SD < 0.04; spectrophotometric method, SD < 0.08. ^{c)} Calculated by CLOGP algorithm [12]; the mean value between the 1*H*- and 2*H*-tautomers is reported. ^{d)} Logarithm of the partition coefficient of the neutral species (SD < 0.03), obtained by potentiometry. ^{e)} Logarithm of the partition coefficient of the ionized species (SD < 0.05), obtained by shake-flask procedure. ^{f)} Obtained by potentiometry. ^{g)} MeOH as co-solvent was used in percentage ranging from 10 to 45; the extrapolation to zero co-solvent was obtained by the Yasuda–Shedlovsky procedure. ^{h)} Validated by shake-flask procedure. ⁱ⁾ Obtained by capillary electrophoresis (CE). ^{j)} Obtained by spectrophotometry.

Table 2. Ionization Constants of Sartans 1–5^{a)}

Compound	$pK_{a1}^{b)}$	Nature ^{c)}	$pK_{a2}^{b)}$	Nature ^{c)}	$pK_{a3}^{b)}$	Nature ^{c)}
1	$3.60 \pm 0.05^d)$	Acidic	$4.70 \pm 0.01^d)$	Acidic	–	–
2	$2.95 \pm 0.05^d)$	Basic	$4.25 \pm 0.04^d)$	Acidic	–	–
3	$3.69 \pm 0.09^d)$	Basic	$4.42 \pm 0.05^d)$	Acidic	–	–
4	$2.12 \pm 0.19^e)$	Basic	$3.34 \pm 0.36^e)$	Acidic	$4.50 \pm 0.24^e)$	Acidic
5	ND ^{d)}		$3.67 \pm 0.04^d)$		$4.66 \pm 0.04^d)$	

^{a)} ND: not determinable (see text for more details). Notation adopted in order of increasing pK_a value.

^{b)} Potentiometric method, SD < 0.09; CE, CI 95% ± 0.36 . ^{c)} Electrical nature of the corresponding pK_a as deduced from the slope of the linear regression obtained by plotting %MeOH vs. pK_a (see Fig. 3).

^{d)} Obtained by potentiometry. ^{e)} Obtained by CE.

$p_s K_a$, the ionization profiles (% of the species against pH), and the lipophilicity profiles are shown in Figs. 3, 4, and 5, respectively.

Valsartan (1). Valsartan contains two acidic centers, the COOH group and the tetrazole ring; as expected, two pK_a values were found potentiometrically (Table 2). By comparison with simpler tetrazoles, the higher value ($pK_{a2} = 4.70$) can be attributed to the prevalent ionization of the tetrazole ring, while the lower ($pK_{a1} = 3.60$) is consequently linked to the prevalent ionization of the COOH group. The lower acidity

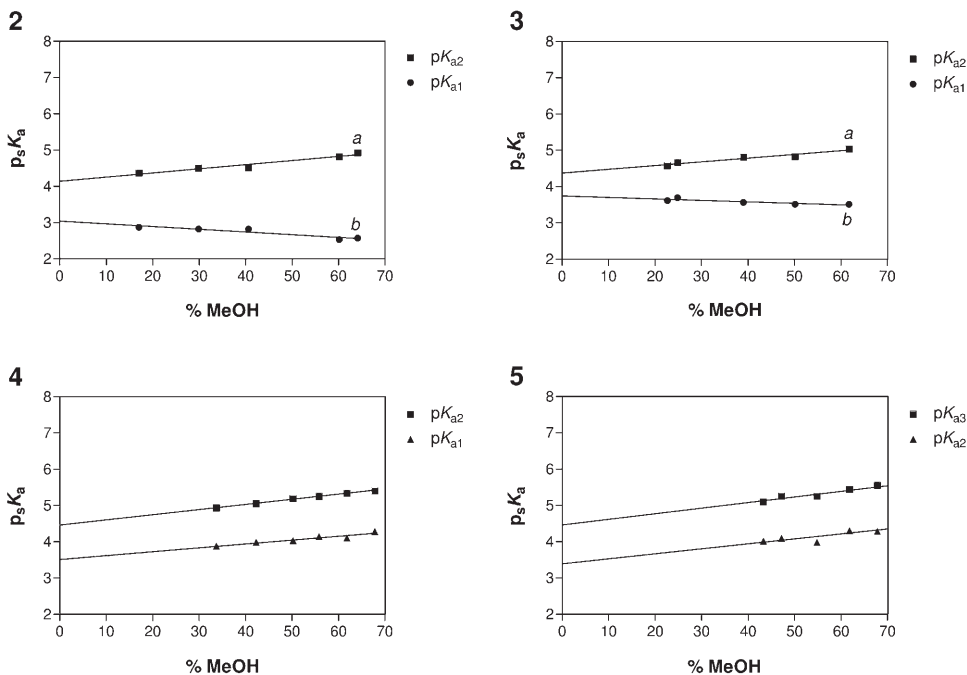


Fig. 3. Plots of weight-% of MeOH vs. $p_s K_a$ for losartan (2), irbesartan (3), candesartan (4), and candesartan cilexetil (5)

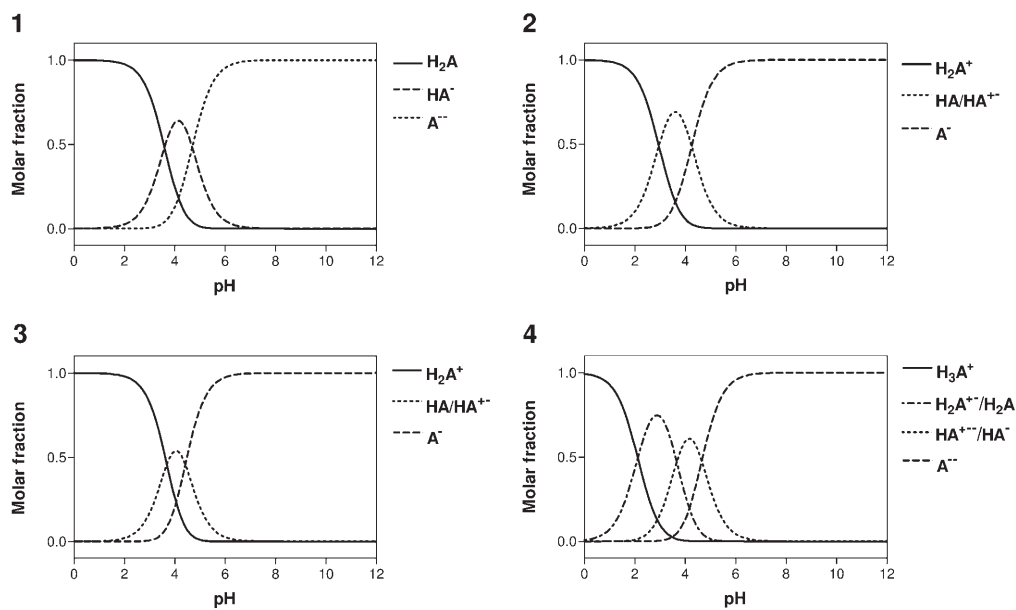


Fig. 4. Ionization profiles (% of the species against pH) of valsartan (1), losartan (2), irbesartan (3), and candesartan (4)

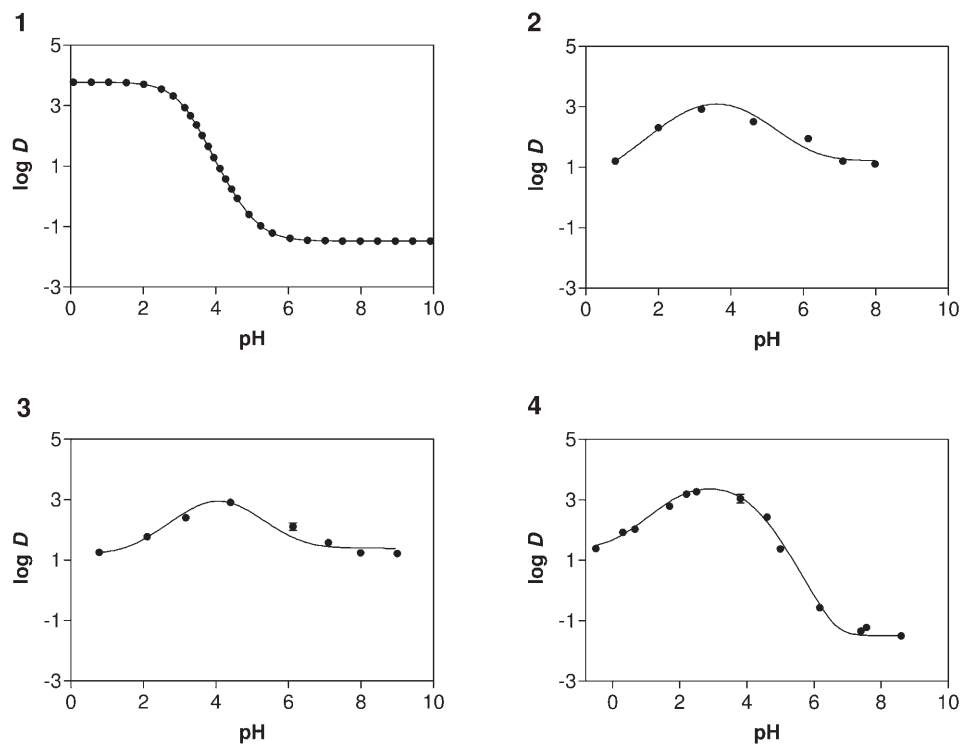


Fig. 5. Lipophilicity profiles of compounds 1–4 obtained by a fitting procedure

with respect to the simple tetrazole **7** can be ascribed to the electrostatic destabilization due to the concomitant negative charge on the COO^- group.

The lipophilicity profile of valsartan (**1**; Fig. 5) displays the pattern typical of a molecule with two acidic centers with close $\text{p}K_{\text{a}}$ values. The ionization profile (Fig. 4) clearly shows that, at $\text{pH} < 1.60$, this drug exists almost exclusively in the undissociated form; thus $\log D^{1.0} = 3.78$ coincides with $\log P^{\text{N}}$, the logarithm of the partition coefficient of the neutral form (H_2A ; Table 3). At $\text{pH} > 6.70$, and thus at physiological pH (blood, 7.4), the drug exists almost exclusively as dianion. Consequently, $\log D^{7.4} = -1.36$ is comparable to $\log P^{2\text{A}}$, *i.e.*, the logarithm of the partition coefficient of the completely ionized form (A^{2-}). The measured partition coefficient of the neutral form ($\log P^{\text{N}}$) is lower than the CLOGP value [12], suggesting a possible hydrophobic collapse between alkyl and aromatic moieties [1], while the *diff* ($\log P^{\text{N}-1}$) parameter ($\log P^{\text{N}} - \log P^{\text{I}} = 5.26$) is compatible with the presence of two negative charges.

Table 3. Lipophilicity Data: Calculated Values and Experimental Results^{a)}

Compound	CLOGP ^{b)}	$\log P^{\text{N}}$ ^{c)}	$\log P^{\text{C}}$ ^{d)}	$\log P^{\text{A}}$ ^{e)}	$\log P^{2\text{A}}$ ^{f)}	$\log D^{7.4}$ ^{g)}	$\log D^{\text{max}}$ ^{h)}
1	4.86	3.78 ⁱ⁾	–	–	–1.48 ⁱ⁾	–1.36 ⁱ⁾	3.78
2	3.85	–	0.85 ^{j)}	1.12 ^{j)}	–	1.16 ^{j)}	3.09
3	6.04	–	1.25 ^{j)}	1.24 ^{j)}	–	1.28 ^{j)}	2.95
4	5.18	–	1.38 ^{j)}	–	–1.50 ^{j)}	–1.35 ^{j)}	3.36

^{a)} Potentiometric data, $\text{SD} < 0.05$; shake flask data, $\text{SD} < 0.1$. ^{b)} Calculated by CLOGP algorithm [12]. ^{c)} Logarithm of the partition coefficient of the neutral species (never present alone except for **1**). ^{d)} Logarithm of the partition coefficient of the cationic species. ^{e)} Logarithm of the partition coefficient of the anionic species (A^-) measured at pH 8.5. ^{f)} Logarithm of the partition coefficient of the dianionic species (A^{2-}) measured at pH 8.5. ^{g)} Logarithm of the apparent partition coefficient at physiological pH. ^{h)} Calculated by fitting procedure. ⁱ⁾ Experimentally obtained by potentiometry (when < 0 validated by shake-flask procedure). ^{j)} Experimentally obtained by shake-flask procedure.

Losartan (2) and Irbesartan (3). Both losartan (**2**) and irbesartan (**3**) contain one acidic center, the tetrazole ring, and one basic center, the imidazole and the 4,5-dihydro-5-oxo-1*H*-imidazole ring, respectively. Two $\text{p}K_{\text{a}}$ values were detected potentiometrically for each of these products. These values indicate a not well-separated dissociation of the protonated basic centre and of the acidic centre ($\Delta\text{p}K_{\text{a}} = 1.30$ and 0.73 for **2** and **3**, resp.). For these two products, the apparent $\text{p}K_{\text{a}}$ values obtained by titration in co-solvent mixtures were plotted against the % composition of the mixtures. Straight lines with a negative slope (known as the typical behavior of basic centers [13]; plots *b* in Fig. 3) were obtained for both products using the apparent constants related to the lower $\text{p}K_{\text{a}}$ values, while lines with a positive slope (known as the typical behavior of acidic centers [13]; plots *a* in Fig. 3) were obtained using the apparent constants related to the higher $\text{p}K_{\text{a}}$ values. Consequently, for compounds **2** and **3**, the lower $\text{p}K_{\text{a}}$ values can be reasonably connected with the prevalent ionization of imidazole ($\text{p}K_{\text{a}1} = 2.95$) and 4,5-dihydro-5-oxo-1*H*-imidazole ($\text{p}K_{\text{a}1} = 3.69$) centers, respectively, while the higher $\text{p}K_{\text{a}}$ values can be ascribed to the prevalent dissociation of the tetrazole centers ($\text{p}K_{\text{a}2} = 4.25$ and $\text{p}K_{\text{a}2} = 4.42$, resp.). The $\text{p}K_{\text{a}}$ assignment for losartan (**2**) and irbesartan

(**3**) further confirms the assignment of the $pK_{a2} = 4.70$ of valsartan (**1**) to the prevalent dissociation of its tetrazole moiety, as proposed above. The ionization profiles deduced from the macroconstants are shown in *Fig. 4*. At physiological pH, the drugs exist principally under the anionic form (A^-). The neutral form in equilibrium with the zwitterionic form is present in a pH-dependent concentration over the pH range 1.0–6.2 for **2** and 1.7–6.4 for **3**. As expected, the lipophilicity behavior of losartan (**2**) and irbesartan (**3**) is quite different from that of valsartan (**1**). These drugs show the classical bell-shaped lipophilicity profile of ordinary ampholytes [14]. This is in keeping with the presence, at $pH < 0.95$ and $pH < 1.69$, respectively, of the hydrophilic cationic forms (H_2A^+ ; **2**, $\log P^C = 0.85$; **3**, $\log P^C = 1.25$), and, at $pH > 6.25$ and $pH > 6.42$, respectively, therefore also at physiological pH, of the sole anionic forms (A^- ; **2**, $\log P^A = 1.12$; **3**, $\log P^A = 1.24$). It should be noted that the $\log D^{\max}$ for **2** and **3** (*Table 3*) at a pH around 3 reflects the lipophilicity of a complex mixture of cationic, anionic, and neutral forms (see distribution profile; *Fig. 5*), while $\log P^N$ cannot be determined; therefore, a direct comparison with the calculated partition coefficients of the neutral forms (CLOGP values) is not feasible.

Candesartan (**4**). A more complex situation occurs with candesartan (**4**). This drug contains two acidic centers (COOH group and tetrazole ring) and one basic center (substituted 1*H*-benzimidazole substructure). Three macroconstant pK_a values were detected for this drug by capillary electrophoresis (CE; *Table 2*). The plot of μ_{eff} vs. pH (*Fig. 6*) shows three partially overlapping inflection points, corresponding to three pK_a values, two acidic and one basic. Indeed, the minimum μ_{eff} value is twofold larger than the maximal μ_{eff} value. The compound exists mainly as a monocationic form (H_3A^+) at pH lower than 0, as zwitterionic and neutral forms (H_2A^{+-} , H_2A) at pH 2.8, as monoanionic forms HA^{+-} and HA^- at pH 4.1, and as a dianionic form (A^{--}) at pH higher than 6.6, thus also at physiological pH. The proximity of the three pK_a values leads to a high value of the 95% confidence intervals for each of them. Only the two higher constants were detectable by the potentiometric method, probably because the third is too low to be measured in the presence of high concentrations of MeOH; it is important to stress that precipitation occurred when less than 45% of MeOH was used. These two constants are reasonably associated, in analogy to valsartan (**1**), to the prevalent dissociation of COOH ($pK_{a2} = 3.67$) and tetrazole ($pK_{a3} = 4.66$) moieties, respectively (*Table 2*). $\Delta pK_a = 0.99$ indicates that the dissociations of these centers are not well-separated. These assignments were confirmed by the plots of the apparent $p_s K_a$ values obtained by potentiometric titration in co-solvent mixtures vs. the % composition of the mixtures (*Fig. 3*; **4**), where straight lines with positive slopes were obtained in the case of the former two centers. Consequently, the lowest pK_a value detected by CE ($pK_{a1} = 2.12$) should be associated to the prevalent ionization of the 1*H*-benzimidazole ring. This assignment is confirmed by the analysis of pK_a values of the 1*H*-benzimidazole models we studied alongside. Actually, the introduction of the EtO substituent at C(2) of 1*H*-benzimidazole (**9**) (\rightarrow **10**) induces a decrease of ca. 1.2 pK units in the basicity. The further introduction of the $PhCH_2$ group at N(1) (\rightarrow **11**) reduces the basicity of additional 0.6 pK units. Finally, **13**, the substructure present in candesartan (**4**), shows basic and acidic pK_a values in keeping with the corresponding pK_a values found in the parent drug. The analysis of the acid–base properties of candesartan (**4**) shows that this drug can exist under several different electrical forms

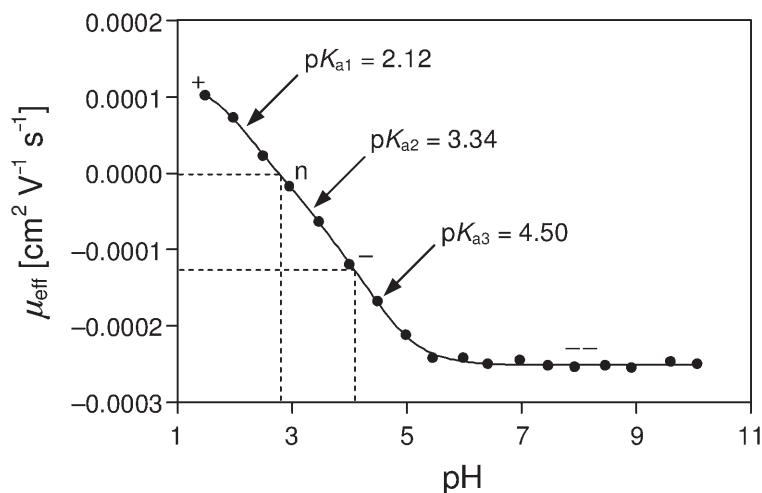


Fig. 6. Relationship between μ_{eff} and pH for candesartan (**4**) in CE experiments. The symbols '+', 'n', '-', and '--' represent the cationic, neutral, monoanionic, and dianionic forms, resp.

(Scheme 1), whose distribution profile, as deduced from the macroconstants, is shown in Fig. 4.

The lipophilicity profile of candesartan (**4**) is complex. At $\text{pH} < 0$, $\log D = 1.38$ represents the lipophilicity of the pure cation (H_3A^+), while, at $\text{pH} > 8$, $\log D = -1.50$ represents the lipophilicity of the dianionic form (A^{--}). The $\log D^{\text{max}}$ occurs at $\text{pH} 3.36$, at which a complex mixture of different forms is present. Certainly, the highly lipophilic neutral form ($\text{CLOGP} = 5.18$) has a great influence on the overall partitioning behavior of the equilibrium mixture. However, the contribution of the other forms cannot be neglected *a priori*, in particular that of zwitterionic species in which intramolecular effects can reduce the hydrophilicity in spite of the presence of two formal charges [14]. To verify this hypothesis, the conformational domain of the two possible zwitterionic forms was explored (see *Exper. Part*). The most stable conformers in a 10-kcal range from the global minimum are shown in Fig. 7. In form *a*, folded conformations are largely preferred, with the protonated 1*H*-benzimidazole center interacting with the anionic tetrazole moiety by a strong charge-enhanced H-bond, so that the interactions with the solvent molecules and the overall hydrophilicity are reduced. In form *b*, the actual separation of opposite formal charges is lowered following delocalization of the positive charge on the 1*H*-benzimidazole nucleus, as evidenced by the distribution of electrostatic potential-derived atom-centered charges on one of the stable conformers (Fig. 8). The behavior of the prodrug candesartan cilxetil (**5**) is particular owing to its ease of hydrolysis to the free acid. Two $\text{p}K_{\text{a}}$ values (one basic and one acidic) were expected for this product. The potentiometric titrations led to the determination of two $\text{p}K_{\text{a}}$ values; the plots of the apparent $\text{p}_s K_{\text{a}}$ values obtained by potentiometric titration in cosolvent mixtures vs. the % composition of the mixtures showed that they are associated to two acidic centers (Fig. 3; **5**). HPLC Stability assays showed that, in aqueous medium, candesartan cilxetil (**5**) is largely hydrolyzed to the parent drug.

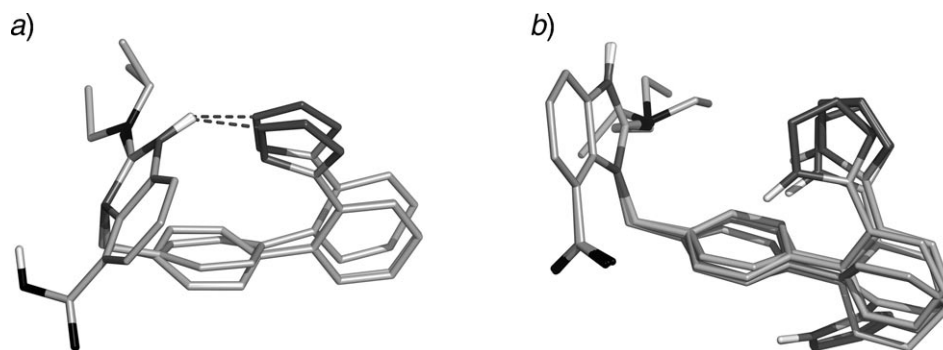


Fig. 7. The most stable conformers in a 10-kcal range from the global minimum for the two zwitterionic forms of candesartan. A charge-enhanced H-bond is represented with a dotted line; non-polar H-atoms have been omitted for clarity.

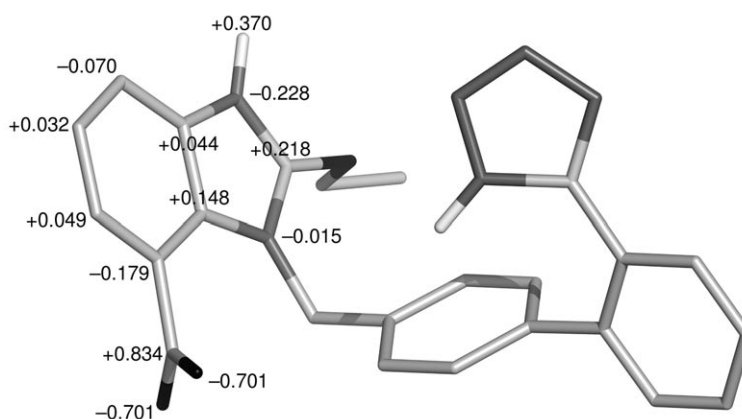


Fig. 8. The distribution of electrostatic potential-derived atom-centered charges on one of the stable conformers of the zwitterionic form b of candesartan. The actual charge separation is lower than the presence of opposite formal charges would suggest: indeed, the carboxylate group bears an overall charge of ca. -0.7 , while the positive charge is largely delocalized over the whole benzimidazole ring. To avoid cluttering the picture, only charges on the benzimidazole nucleus have been reported.

Therefore, the pK_a values determined by potentiometric titration are essentially the pK_a values of candesartan (**4**). The same picture was found when the CE method was used. By contrast, no hydrolysis was observed with the simple methyl *1H*-benzimidazole-carboxylate **12**, whose basic pK_a value was near that of candesartan (**4**). This similarity is conceivably due to two reasons: first, the COOH group of **4** is largely present in the unionized form when the pK_a associated to the benzimidazole substructure is measured; second, the electronic effects of COOH and COOMe groups are similar [15]. The ease of hydrolysis and low solubility of candesartan cilexetil (**5**) prevented the investigation of its lipophilicity profile.

Conclusions. – pH-Dependent partition profiles and pK_a values of some important sartan drugs were determined. The combined use of the potentiometric and CE methods allowed the complete determination of all pK_a values. The analysis of cosolvent weight-% vs. $p_s K_a$ plots and the study of the ionization of appropriate model compounds allowed the assignment of all measured pK_a values to specific ionizable moieties of the drugs. The pH-dependent partition profiles should provide good descriptors for studies of relationships between structure and distribution of the drugs. At physiological pH, losartan (**2**) and irbesartan (**3**) exist principally in the anionic form, while valsartan (**1**) and candesartan (**4**) are present mainly in their dianionic form. The study of candesartan cilexetil (**5**) was complicated by both the facility with which the prodrug undergoes hydrolysis and its low solubility in H_2O .

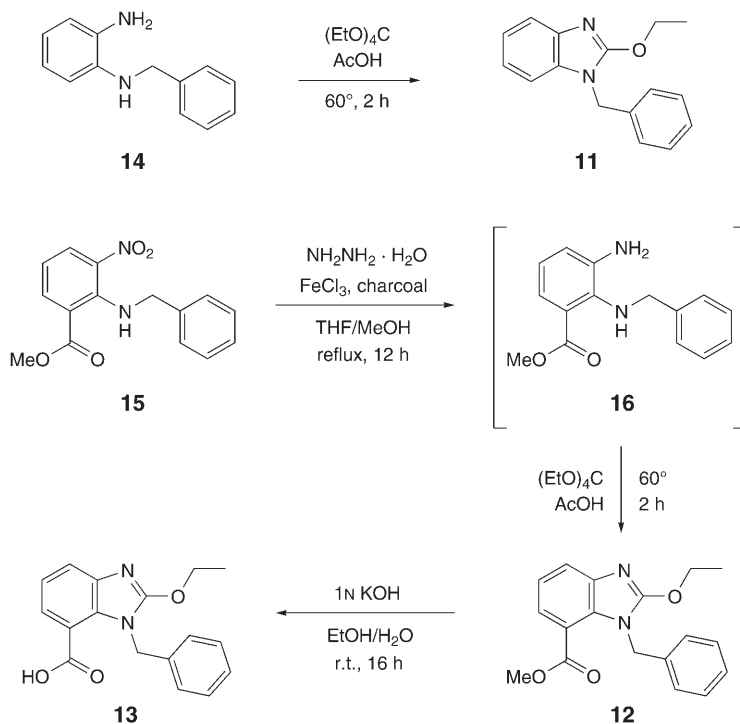
This work was supported by a MIUR grant (COFIN 2005).

Experimental Part

General. Sartans **1–5** were kindly supplied by different pharmaceutical companies: valsartan (**1**) by Novartis Farma (I-Origgio), losartan (**2**) by Merck Sharp & Dohme (I-Roma), irbesartan (**3**) by Sanofi Synthelabo (I-Limito), candesartan (**4**) and candesartan cilexetil (**5**) by Astra Zeneca (I-Milano). Octanol was of spectrophotometric grade (*Sigma-Aldrich*), and MeOH was of HPLC-grade (*Carlo-Erba*). Compounds **6** [16], **7** [17], and **10** [9] were synthesized according to literature, while **8** and **9** were purchased from *Sigma-Aldrich*. Compound **11** was prepared starting from **14**, and compounds **12** and **13** were prepared starting from **15** via **16** (Scheme 2). Flash column chromatography (FC): silica gel (*Merck, Kieselgel 60*, 230–400 mesh ASTM); PE stands for 40–70° petroleum ether. The progress of the reactions was followed by TLC (5 × 20-cm plates with a layer thickness of 0.2 mm). Anhydrous $MgSO_4$ was used as drying agent for the org. phases. Org. solvents were removed under vacuum at r.t. M.p.: cap. apparatus (*Büchi 540*). 1H - and ^{13}C -NMR spectra: *Bruker Avance-300* at 300 and 75 MHz, resp., with Me_4Si as the internal standard; δ in ppm, J in Hz. Low-resolution (LR) MS: *Finnigan Mat-TSQ-700*; in m/z . The results of elemental analyses (C, H, N) for the new 1*H*-benzimidazole derivatives are within $\pm 0.4\%$ of the theoretical values (*REDOX*, I-Monza).

*1-Benzyl-2-ethoxy-1*H*-benzimidazole (11).* AcOH (0.25 ml, 4.4 mmol) was added to a soln. of *N*-benzylbenzene-1,2-diamine (**14**) [18]; 0.87 g, 4.4 mmol) in $(EtO)_4C$ (4.0 ml, 19 mmol). The mixture was heated at 60° for 2 h; after cooling, Et_2O was added (30 ml), and the org. layer was washed with 10% $NaHCO_3$ (3 × 15 ml), then with brine (10 ml), dried, and evaporated. The crude product was purified by FC (PE/AcOEt 9:1), then recrystallized from hot iPr_2O /hexane to give **11** (0.93 g, 84%). White solid. M.p. 69.5° (iPr_2O /hexane). 1H -NMR ($(D_6)DMSO$): 7.43–7.03 (*m*, 9 H); 5.22 (*s*, 2 H); 4.56 (*q*, $J = 7.05$, 2 H); 1.39 (*t*, $J = 7.05$, 3 H). ^{13}C -NMR ($(D_6)DMSO$): 156.7; 139.8; 136.7; 133.3; 128.6; 127.5; 127.1; 121.0; 120.5; 117.0; 109.0; 65.9; 44.7; 14.4. CI-MS: 253 ($[M + 1]^+$). Anal. calc. for $C_{16}H_{16}N_2O$ (252.31): C 76.16, H 6.39, N 11.10; found: C 76.00, H 6.32, N 11.06.

*Methyl 1-Benzyl-2-ethoxy-1*H*-benzimidazole-7-carboxylate (12).* $FeCl_3 \cdot 6 H_2O$ (0.013 g, 0.05 mmol) and activated charcoal (0.13 g, 11 mmol) were added to a soln. of methyl 2-(benzylamino)-3-nitrobenzoate (**15**) [19]; 1.0 g, 3.5 mmol) in a mixture of MeOH (15 ml) and freshly distilled THF (15 ml), according to a known procedure [20]. After refluxing for 30 min, a soln. of $NH_2NH_2 \cdot H_2O$ (1.04 ml, 21 mmol) in MeOH (15 ml) was added dropwise to the mixture over 10 min. The resulting mixture was refluxed for further 14 h; after cooling, the insoluble material was removed by filtration through a *Celite* pad, washing the filter thoroughly with CH_2Cl_2 (100 ml). The filtrate was washed with 10% $NaHCO_3$ (3 × 20 ml), then with brine (10 ml), dried, and evaporated. The residue was dissolved in $(EtO)_4C$ (5.0 ml, 24 mmol), then AcOH was added (0.20 ml, 3.5 mmol). The mixture was heated at 60° for 2 h; after cooling, Et_2O was added (30 ml), and the org. layer was washed with 10% $NaHCO_3$ (3 × 15 ml), then with brine (10 ml), dried, and evaporated. The crude product was purified by FC (PE 9/AcOEt 1), then recrystallized from hot iPr_2O /hexane to give **12** (0.65 g, 60%). White solid. M.p. 114° (iPr_2O /

Scheme 2. Synthetic Route to Derivatives **11–13**

hexane). $^1\text{H-NMR}$ ((D_6) DMSO): 7.71–7.69 (*m*, 1 H); 7.45–7.42 (*m*, 1 H); 7.29–7.16 (*m*, 4 H); 6.93–6.90 (*m*, 2 H); 5.49 (*s*, 2 H); 4.61 (*q*, $J = 7.05$, 2 H); 1.40 (*t*, $J = 7.05$, 3 H). $^{13}\text{C-NMR}$ ((D_6) DMSO): 166.0; 158.3; 141.6; 136.8; 128.4; 127.1; 126.1; 120.7; 115.4; 66.5; 52.1; 46.4; 40.0; 39.7; 39.4; 39.1; 38.9; 38.6; 14.3. CI-MS: 311 ($[M + 1]^+$). Anal. calc. for $\text{C}_{18}\text{H}_{18}\text{N}_2\text{O}_3$ (310.35): C 69.66, H 5.85, N 9.03; found: C 69.49, H 5.87, N 9.05.

1-Benzyl-2-ethoxy-1H-benzimidazole-7-carboxylic acid (13). Compound **12** (0.30 g, 0.97 mmol) was dissolved in 20 ml of ethanolic 1N KOH and stirred for 16 h. The mixture was then diluted with H_2O (20 ml), the solvent was evaporated, and the aq. phase was washed with Et_2O (3×15 ml), then pH was adjusted to 5 with 37% HCl. The precipitate was collected by filtration, washed with H_2O , and dried (P_2O_5). The crude product was recrystallized from hot THF/ Pr_2O to give **13** (0.17 g, 60%). White solid. M.p. 177.5° (THF/ Pr_2O). $^1\text{H-NMR}$ ((D_6) DMSO): 7.72–7.62 (*m*, 1 H); 7.55–7.47 (*m*, 1 H); 7.32–7.10 (*m*, 4 H); 7.02–6.90 (*m*, 2 H); 5.62 (*s*, 2 H); 4.61 (*m*, 2 H); 1.39 (*m*, 3 H). $^{13}\text{C-NMR}$ ((D_6) DMSO): 167.4; 158.2; 141.6; 137.4; 128.5; 127.1; 126.4; 120.6; 116.7; 66.4; 46.4; 40.0; 39.8; 39.5; 39.2; 38.9; 38.6; 14.3. CI-MS: 297 ($[M + 1]^+$). Anal. calc. for $\text{C}_{17}\text{H}_{16}\text{N}_2\text{O}_3$ (296.32): C 68.91, H 5.44, N 9.45; found: C 69.15, H 5.52, N 9.49.

Determination of Ionization Constants. Ionization constants of compounds **1–5**, as well as of tetrazole and of benzimidazole model compounds, *i.e.*, **6–8** and **9–13**, resp., were determined by potentiometry, capillary electrophoresis (CE), and UV spectrophotometry, according to the need (see *Results and Discussion*). Potentiometric titrations were carried out with a *GLpKa* apparatus (*Sirius Analytical Instruments Ltd.*, Forrest Row, East Sussex, UK). Apparent ionization constants ($\text{p}K_a$) were obtained in co-solvent mixtures because of the low solubility of compounds in H_2O . MeOH is the solvent of choice for this purpose, because its general effects on $\text{p}K_a$ values have been extensively studied [13]. At least five different hydro-organic solns. (ionic strength adjusted to 0.15M with KCl) of the compounds

(20 ml, *ca.* 1 mM in 15–68 wt-% MeOH) were initially acidified to pH 1.8 with 0.5N HCl. The solns. were then titrated with standardized 0.5N KOH to pH 10.5. The titrations were performed under Ar at $25.0 \pm 0.1^\circ$. The initial estimates of the $p_s K_a$ values (the apparent ionization constants in the H₂O/MeOH mixtures) were obtained by *Bjerrum* plots; these values were finally refined by a weighted nonlinear least-squares procedure. Aqueous pK_a values were obtained by extrapolation using the *Yasuda–Shedlovsky* (*Y–S*) procedure (*Eqn. 1*) [13]:

$$p_s K_a + \log [H_2O] = A \cdot 1/\epsilon + B \quad (1)$$

where $[H_2O]$ is the molar H₂O concentration, and ϵ is the dielectric constant of the mixture (55.5 and 78.3, resp., for pure water), A and B are the coefficients of the linear regression. The plot of wt-% of MeOH vs. $p_s K_a$ (*Y–S* plot) was drawn for each compound in order to allow the correct assignment of the electrical nature for the different ionization sites.

Spectrophotometric measurements were carried out at 25° with a UV/VIS spectrophotometer (*UV-2501PC*, *Shimadzu*) according to [21]. Absorbance spectra of compounds (*ca.* 100 μ M) were recorded from 220 to 360 nm in several buffers at a constant ionic strength of 50 mM (pH range 0.0 to 8.0 with increments of 0.5 pH units); absorption readings were made at selected wavelengths which maximize the difference of absorption between the ionized and the unionized form. For each compound, at least six pK_a values at different pHs were measured.

CE Experiments were performed with an *HP^{3D}CE* system (*Agilent Technologies*, D-Waldbronn) equipped with an on-column diode-array detector, an autosampler, and a power supply able to deliver up to 30 kV. The separation was performed in a fused silica capillary (*BGB Analytik*, CH-Böckten) with an inner diameter of 50 μ m and 32.5 cm total length (24 cm to the UV detector). Samples were introduced by short-end injection: polarity was reversed and samples were injected at the detector side, thus reducing the effective length from 24 to 8.5 cm. An injection equivalent to 1.5% of the effective length was performed by applying a pressure of 12 mbar for 4 s. During analysis, a voltage of 2 to 8 kV was applied in order to avoid the *Joule* effect. The capillary was thermostated at 25° by a high-velocity air stream. UV Detection was carried out at 210 nm for sartans and benzimidazole models, and at 260 nm for acetone. A two-stage dynamic coating procedure using *Ceofix* (*Analisis*, B-Namur) was applied to generate a large and constant electroosmotic flow (EOF) at any pH. Samples were freshly prepared every day. They were set at a concentration of 100 ppm in 5% acetone (EOF neutral marker). Up to 40% MeCN was added to some sample solns. to enhance compound solubility. Eighteen buffers were prepared from pH 1.5 to 10.0 with increments of 0.5 pH units; they were set at a constant ionic strength of 50 mM. Each compound was injected once at every pH value. The analysis time was lower than 5 min. Effective mobility (μ_{eff}) was calculated from the migration times of the analyte and neutral marker. Calculated μ_{eff} values were reported as a function of pH, giving rise to a sigmoidal curve. Nonlinear regression (*GraphPad Prism 4.02*, *GraphPad Software*, San Diego, CA; USA) was accomplished to determine apparent pK_a values [22][23].

Determination of Lipophilicity Profiles. For valsartan (**1**), lipophilicity data were obtained by the potentiometric method. At least four different titrations (*ca.* 1 mM) were carried out in a pH range from 1.8 to 12.2, using various volumes of octanol (volume ratios of org. solvent/H₂O ranging from 0.05 to 1). The titrations were carried out under Ar at $25.0 \pm 0.1^\circ$. In the presence of octanol, the pK_a value shifts, giving an apparent constant called $p_0 K_a$; this shift is due to the partitioning of the substance into the org. phase. The shifts in pK_a values are used to determine $\log P^N$ and $\log P^I$ (the logarithm of the partition coefficient of the neutral and the ionized form, resp.). The details of the method have been reported in [24].

Due to the complex ionization profile of losartan (**2**), irbesartan (**3**), and candesartan (**4**), the apparent partition coefficients ($\log D^{pH}$) were measured by the shake-flask procedure according to [25]. Several 0.05M buffers were chosen according to the required pH (pH 0.0 to 8.5); ionic strength was adjusted to 0.15M with KCl. Octanol was added to the buffers, and the two phases were mutually saturated by shaking for 4 h. The compounds were solubilized in the buffered aq. phase at a concentration of *ca.* 0.1 mM, and an appropriate amount of octanol was added. The two phases were shaken for *ca.* 20 min, by which time the partitioning equilibrium of solutes is reached, and then centrifuged

(10000 rpm, 10 min). The concentration of the solutes in the aq. phase was measured by UV spectrophotometry (*UV-2501PC*, *Shimadzu*) at λ_{\max} . For each compound, at least seven log D values at different pHs were measured. The distribution profiles were obtained by a fitting procedure using Eqn. 2:

$$D = \sum f^i \cdot P^i \quad (2)$$

where D is the distribution coefficient, f^i is the molar fraction of the electrical species i and P^i is the partition coefficient of i . The molar fractions were calculated using the experimental pK_a values.

The potentiometric method described above for valsartan (**1**) was adopted to assess the log P^N values of reference tetrazoles **6–8**, while log P^I , which could be determined only for the two most lipophilic aromatic terms **7** and **8**, was measured by the shake-flask procedure.

Conformational Study. The molecular models of the two zwitterionic forms of **4** were constructed using standard bond lengths and angles with the MOE software package [26]. The ground-state geometries were fully optimized without geometry constraints according to the AM1 semiempirical method until the largest component of the gradient was less than $1 \cdot 10^{-4}$ Hartree Bohr⁻¹. All quantum-mechanical calculations were accomplished with the GAMESS-US software package [27]. The conformational space of the selected models was explored with MOE by means of quenched molecular dynamics (QMD), since this method has been reported to be the most appropriate to find highly diverse conformers characterizing the partitioning behavior of org. molecules [28]. 200 5-ps MD simulations were performed *in vacuo* at 600 K with the MMFF94 force field, starting from the AM1 geometries with a Boltzmann distribution of the atomic velocities (time step 1 fs). At the end of every 5-ps trajectory, the final conformer was minimized through a truncated Newton–Raphson geometry optimization until the gradient was less than 0.001 kcal mol⁻¹, then stored in a database, and used as the starting geometry for the subsequent QMD cycle. At the end of the run, duplicate conformers were eliminated from the database according to the criteria proposed in [28]. The whole QMD procedure was repeated five times for each model in order to ensure thorough sampling of the conformational space; at the end of all runs, the same results were found. To ensure a reliable estimation of the relative energies, as well as of the electrostatic potential, all conformers underwent an additional AM1 optimization followed by a single-point energy evaluation with a DFT method, using the RB3LYP/6-311 + G(2d,2p) basis set. Atom-centered charges were fit to the *ab initio* electrostatic potential according to the RESP procedure as implemented in AMBER 9 [29]. All calculations were run on a Linux cluster composed of 24 CPUs (*Pentium IV* single core, clock frequency ranging from 1.6 to 3.2 GHz).

REFERENCES

- [1] P.-A. Carrupt, B. Testa, P. Gaillard, *Rev. Comput. Chem.* **1997**, *11*, 241.
- [2] R. A. Conradi, P. S. Burton, R. T. Borchardt, in ‘Lipophilicity in Drug Action and Toxicology’, Eds. V. Pliška, B. Testa, H. van de Waterbeemd, VCH, Weinheim, 1996, p. 233–252.
- [3] V. Pliška, in ‘Lipophilicity in Drug Action and Toxicology’, Eds. V. Pliška, B. Testa, H. van de Waterbeemd, VCH, Weinheim, 1996, p. 263–294.
- [4] E. K. Jackson, in ‘Goodman and Gilman’s. The Pharmacological Basis of Therapeutics’, Eds. J. G. Hardman, L. E. Limbird, McGraw-Hill, New York, 2001, p. 8009–8042.
- [5] E. Cagigal, L. González, R. M. Alonso, R. M. Jiménez, *J. Pharm. Biomed. Anal.* **2001**, *26*, 477.
- [6] T. Eicher, S. Hauptmann, ‘The Chemistry of Heterocycles’, Thieme, New York, 1995.
- [7] V. A. Ostrovskii, G. I. Koldobskii, N. P. Shirokova, V. S. Poplavskii, *Chem. Heterocycl. Compd. (Engl. Transl.)* **1981**, *17*, 412.
- [8] L. D. Hansen, E. J. Baca, P. Scheiner, *J. Heterocycl. Chem.* **1970**, *7*, 991.
- [9] D. J. Brown, R. K. Lynn, *J. Chem. Soc., Perkin Trans. 1* **1974**, 349.
- [10] G. Caron, F. Reymond, P.-A. Carrupt, H. H. Girault, B. Testa, *Pharm. Sci. Technol. Today* **1999**, *2*, 327.
- [11] G. Bouchard, P.-A. Carrupt, B. Testa, V. Gobry, H. H. Girault, *Chem. – Eur. J.* **2002**, *8*, 3478.
- [12] Bio-Loom for Windows, v. 1.5, *BioByte Corporation*, Claremont, CA, USA.

- [13] A. Avdeef, J. E. A. Comer, S. J. Thomson, *Anal. Chem.* **1993**, *65*, 42.
- [14] A. Pagliara, P.-A. Carrupt, G. Caron, P. Gaillard, B. Testa, *Chem. Rev.* **1997**, *97*, 3385.
- [15] O. Exner, in 'Correlation Analysis in Chemistry', Eds. N. B. Chapman, J. Shorter, Plenum Press, New York, 1978, p. 439–540.
- [16] W. Ogilvie, W. Rank, *Can. J. Chem.* **1987**, *65*, 166.
- [17] W. G. Finnegan, R. A. Henry, R. Lofquist, *J. Am. Chem. Soc.* **1958**, *80*, 3908.
- [18] P. Chattopadhyay, R. Rai, P. S. Pandey, *Synth. Commun.* **2006**, *36*, 1857.
- [19] J. W. Hubbard, A. M. Piegols, B. C. G. Söderberg, *Tetrahedron* **2007**, *63*, 7077.
- [20] K. Kubo, Y. Kohara, E. Imamiya, Y. Sugiura, Y. Inada, Y. Furukawa, K. Niahikawa, T. Naka, *J. Med. Chem.* **1993**, *36*, 2182.
- [21] A. Albert, E. P. Serjeant, 'The determination of ionization constants', 3rd edn., Chapman and Hall, London, 1984.
- [22] L. Geiser, Y. Henchoz, A. Galland, P.-A. Carrupt, J.-L. Veuthey, *J. Sep. Sci.* **2005**, *28*, 2374.
- [23] Y. Henchoz, J. Schappler, L. Geiser, J. Prat, P.-A. Carrupt, J.-L. Veuthey, *Anal. Bioanal. Chem.* **2007**, *389*, 1869.
- [24] A. Avdeef, *Quant. Struct.-Act. Relat.* **1992**, *11*, 510.
- [25] J. C. Dearden, G. M. Bresnen, *Quant. Struct.-Act. Relat.* **1988**, *7*, 133.
- [26] MOE version 2006.08, *Chemical Computing Group Inc.*, Montreal, Quebec, Canada.
- [27] M. W. Schmidt, K. K. Baldrige, J. A. Boatz, S. T. Elbert, M. S. Gordon, J. H. Jensen, S. Koseki, N. Matsunaga, K. A. Nguyen, S. J. Su, T. L. Windus, M. Dupuis, J. A. Montgomery, *J. Comput. Chem.* **1993**, *14*, 1347.
- [28] C. Altomare, S. Cellamare, A. Carotti, G. Casini, M. Ferappi, E. Gavuzzo, F. Mazza, P.-A. Carrupt, P. Gaillard, B. Testa, *J. Med. Chem.* **1995**, *38*, 170.
- [29] J. Wang, P. Cieplak, P. A. Kollman, *J. Comput. Chem.* **2000**, *21*, 1049.

Received November 27, 2007